Gas Turbine Performance and Health Status Estimation Using Adaptive Gas Path Analysis

Y. G. Li
School of Engineering,
Cranfield University,
Bedford MK43 0AL, UK

In gas turbine operations, engine performance and health status are very important information for engine operators. Such engine performance is normally represented by engine airflow rate, compressor pressure ratios, compressor isentropic efficiencies, turbine entry temperature, turbine isentropic efficiencies, etc., while the engine health status is represented by compressor and turbine efficiency indices and flow capacity indices. However, these crucial performance and health information cannot be directly measured and therefore are not easily available. In this research, a novel Adaptive Gas Path Analysis (Adaptive GPA) approach has been developed to estimate actual engine performance and gas path component health status by using gas path measurements, such as gas path pressures, temperatures, shaft rotational speeds, fuel flow rate, etc. Two steps are included in the Adaptive GPA approach, the first step is the estimation of degraded engine performance status by a novel application of a performance adaptation method, and the second step is the estimation of engine health status at component level by using a new diagnostic method introduced in this paper, based on the information obtained in the first step. The developed Adaptive GPA approach has been tested in four test cases where the performance and degradation of a model gas turbine engine similar to Rolls-Royce aero engine Avon-300 have been analyzed. The case studies have shown that the developed novel linear and nonlinear Adaptive GPA approaches can accurately and quickly estimate the degraded engine performance and predict the degradation of major engine gas path components with the existence of measurement noise. The test cases have also shown that the calculation time required by the approach is short enough for its potential online applications. [DOI: 10.1115/1.3159378]

Keywords: gas turbine engine, performance adaptation, gas path diagnostics, Adaptive GPA

1 Introduction

With the development of thermodynamic modeling techniques and softwares, performance simulation of gas turbine engines becomes a quick and reliable tool for gas turbine engineers to analyze engine performance. During gas turbine operation, however, the deviation of gas turbine performance is indicated by the deviation of gas path measurements, such as gas path pressures, temperatures, shaft rotational speeds, fuel flow rate, etc. Such performance deviation may be due to varying ambient and operating conditions or engine performance degradations associated with prolonged operation time and hostile operating environment. Normally, gas turbine engine performance is represented by engine performance parameters such as airflow rate, compressor pressure ratios, compressor isentropic efficiencies, turbine entry temperature, combustor combustion efficiency, turbine isentropic efficiencies, etc., while engine performance health is represented by engine health parameters such as compressor and turbine isentropic efficiency indices and flow capacity indices. Gas turbine engine performance and engine health status may not be directly measured and therefore are not easily visible to engine operators. Interpretation of the deviation of engine performance and health status relative to its initial condition by using gas path performance analysis techniques is very important to both engine operators and designers alike.

Some techniques have been developed in the past in the field of gas turbine engine performance matching or adaptation. Roth et al. [1] introduced an optimization concept for an engine cycle model matching and a minimum variance estimator algorithm [2] for performance matching of a turbofan engine. Li et al. [3] introduced an adaptation matrix manipulation method and genetic algorithm adaptation method [4] for gas turbine design point performance adaptation and successfully applied the methods to the test data of an industrial gas turbine engine. Many gas path diagnostic methods have been developed in the past and the typical ones are Gas Path Analysis (GPA) and its derivatives [5–12], neural networks [13–15], Bayesian belief networks [16], genetic algorithm [17–19], fuzzy logic [20–22], diagnostics using transient measurements [23,24], etc. More comprehensive reviews on gas turbine gas path diagnostic techniques were given by Li [25], Singh [26], and Jaw [27].

In this paper, a novel gas turbine engine performance and health status estimation approach, called Adaptive Gas Path Analysis (Adaptive GPA), has been developed. It uses the gas path measurements as input information to estimate changing engine performance and degraded health of major engine gas path components. The developed approach is applied to a model gas turbine engine similar to Rolls-Royce aero engine Avon-300 implanted with different component degradations to test the effectiveness of the approach. Analysis and conclusions are made accordingly.

2 Adaptive GPA

Engine performance status is represented by engine component performance parameters, such as engine airflow rate, bypass ratio, compressor pressure ratios, compressor isentropic efficiencies, combustor combustion efficiency, turbine entry temperature, tur-

Contributed by the International Gas Turbine Institute of ASME for publication in the JOURNAL OF ENGINEERING FOR GAS TURBINES AND POWER. Manuscript received March 23, 2009; final manuscript received March 26, 2009; published online January 25, 2010. Review conducted by Dilip R. Ballal. Paper presented at the ASME Gas Turbine Technical Congress and Exposition, Orlando, FL, June 8–12, 2009.

bine isentropic efficiencies, thrust, specific fuel consumption (SFC), etc. Engine performance degradation is represented by component health parameters, i.e., compressor and turbine efficiency indices and flow capacity indices, and has great impact on engine component performance as well as whole engine performance. The change in ambient condition, operating condition, and engine health has a significant impact on engine performance. Correspondingly, the engine will reach a new thermodynamic equilibrium condition, and gas path measurements of the engine, such as gas path pressures, temperatures, rotational speeds, fuel flow rate, etc., will deviate from their original values. A novel approach has been developed and is named as Adaptive GPA whose objective is to estimate the deviated engine performance and also determine the engine component degradation based on the deviation of gas path measurements. Such Adaptive GPA approach is divided into two steps: The first step is the estimation of deviated engine performance based on gas path measurements, and the second step is the estimation of engine degradation by assessing each component health condition at component level. The following are the detailed descriptions of the Adaptive GPA approach.

2.1 Performance Status Estimation. As the first step of the Adaptive GPA, the performance status estimation is to assess actual deviated engine performance due to engine degradation based on measured gas path parameters. Although degraded engine performance is an off-design performance, once reaching a thermodynamic equilibrium condition, an engine condition can be regarded as an artificial design point, and its performance can be predicted using a design point performance adaptation method. Several design point performance matching or adaptation methods have been developed in the past by different researchers [1–4], and any one of them may be used to achieve the objective of the first step of the Adaptive GPA. The performance adaptation method used in this study is the one reported in Ref. [3] developed by the same author of this paper to estimate the actual engine performance at a degraded condition. Due to that such performance estimation is an essential step toward the degradation estimation in the second step, it is described briefly as follows to assist readers to understand the whole idea of the Adaptive GPA.

The thermodynamic relationship between engine gas path measurement and engine component performance parameters can be represented with Eq. (1), assuming that the ambient and operating conditions are unchanged.

$$\vec{z} = h(\vec{x}) \tag{1}$$

where $\vec{z} \in R^M$ is the gas path measurement parameter vector, M is the number of measurement parameters, $\vec{x} \in R^N$ is the component performance parameter vector, N is the number of component performance parameters, and $h(\,)$ is a vector valued function representing engine thermodynamic relationship between $\vec{x}$ and $\vec{z}$. If the measurements are obtained at slightly different ambient and operating conditions, the measurement data should be corrected to the same ambient and operating conditions before the data can be used.

When an engine is clean (i.e., undegraded) and operates at a specified operating condition, the performance status of the engine is denoted by subscript "0". If the engine operates at a slightly deviated condition due to engine degradation, the engine performance represented with Eq. (1) can be expanded in a Taylor series expansion around condition 0, assuming that the engine performance deviation is small,

$$\vec{z} = \vec{z}_0 + \left.\frac{\partial h(\vec{x})}{\partial \vec{x}}\right|_0 (\vec{x} - \vec{x}_0) + \text{HOT} \tag{2}$$

where HOT is the higher order terms of the expansion and can be neglected when the performance deviation is small. Therefore, a linearized gas turbine performance model can be expressed with Eq. (3).

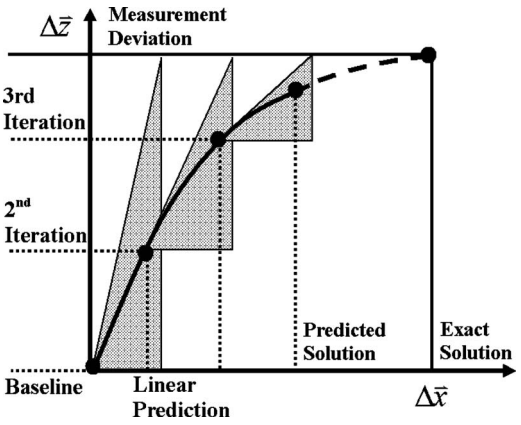

Fig. 1 Nonlinear Newton–Raphson method [11]

$$\Delta\vec{z} = H \cdot \Delta\vec{x} \tag{3}$$

The deviation of component performance parameters can be predicted by inverting the influence coefficient matrix (ICM) H to an adaptation coefficient matrix (ACM) H^{-1}, leading to Eq. (4) when $M=N$.

$$\Delta\vec{x} = H^{-1} \cdot \Delta\vec{z} \tag{4}$$

Then the deviated engine performance status can be estimated with Eq. (5)

$$\vec{x} = \vec{x}_0 + \Delta\vec{x} \tag{5}$$

where $\vec{x}_0$ is the original engine component performance parameter vector, while $\Delta\vec{x}$ is the deviation of component performance parameter vector indicated by the change in gas path measurements $\Delta\vec{z}$. The method described above is called linear performance adaptation approach.

To ensure a unique solution of performance adaptation, it is required that the number of gas path measurement parameters M should be no less than the number of component performance parameters N, i.e.,

$$M \geq N \tag{6}$$

If $M>N$, i.e., there are redundant measurement parameters compared with the number of component performance parameters, and Eq. (3) is overdetermined. When that happens, a pseudoinverse of H is

$$H^{\#} = (H^T H)^{-1} H^T \tag{7}$$

and the resulting solution $\vec{x}=H^{\#}\vec{z}$ of Eq. (3) is the best in a least-squares sense.

Due to that the engine performance may deviate nonlinearly from its initial baseline condition because of nonlinear thermodynamic behavior of engine performance, the linear performance adaptation may not be able to provide accurate estimation of engine performance deviation. Therefore an iterative process, a Newton–Raphson method, is introduced to improve the accuracy of the estimation where linear adaptation is applied iteratively until a converged solution is obtained [11] (Fig. 1). The above method is called the nonlinear performance adaptation. Theoretically, the nonlinear performance adaptation has the potential to provide better adaptation results than its linear partner.

The convergence of the nonlinear performance adaptation process shown in Fig. 1 is declared when the predicted measurement parameters are very close to the actual measurement parameters. This criterion is shown in Eq. (8) where the root mean square (rms) of the difference between the predicted and actual measurement parameters is smaller than σ when convergence is declared:

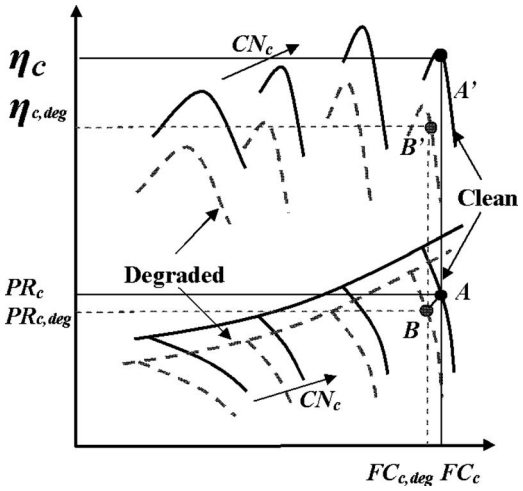

Fig. 2 Compressor characteristic map

$$\text{rms} = \sqrt{\frac{\sum_{i=1}^{M}[(z_{i,\text{predicted}} - z_{i,\text{actual}})/z_{i,\text{actual}}]^2}{M}} < \sigma \tag{8}$$

where σ is a very small number (σ=0.001 in this study).

Such performance status estimation method is fast in computation speed, and the accuracy of the estimation is mainly determined by the accuracy of the gas path measurements.

Although different gas turbine design point performance adaptation methods [1–4] have been developed, this is the first time one of these methods is introduced to estimate performance status of a degraded engine. Such estimation method has the advantage that it does not need any component characteristic maps. As the result of the performance status estimation, the deviated engine performance due to engine degradation can be predicted.

2.2 Engine Health Status Estimation. Once the degraded performance of an engine is obtained, it can be compared with the initial engine performance when the engine was new. Such comparison can be done at a component level by comparing the operating point of each component on its characteristic map when the component is degraded with the operating point on the same map when the component is not degraded. This leads to the estimation of degradation of every major engine component of compressors, combustors, and turbines. To assist the analysis of gas turbine degradation, it is assumed that the degraded characteristic maps of compressors, combustors, and turbines will keep more or less the same shape as their original maps, based on the fact that their geometries do not change significantly after they are degraded. The degradation of the components is represented by the shift of the characteristic curves on the maps, and such shift is represented by degradation indices to be discussed later.

The detailed procedure of such idea forms the second step of the Adaptive GPA, and its detailed approach is the major contribution of this paper described in detail as follows.

2.2.1 Compressor Degradation Estimation. Most open literature has only mentioned compressor degradation represented by two degradation parameters relevant to compressor isentropic efficiency and flow capacity. However, the degradation of a compressor may be described more realistically by the deviation of three degradation indices relevant to its isentropic efficiency, flow capacity, and pressure ratio. A typical compressor characteristic map is shown in Fig. 2 where the relationship among four compressor characteristic parameters, i.e., pressure ratio PR_c, isentropic efficiency η_c, flow capacity FC_c, and relative rotational speed CN_c, at different operating conditions is represented. In the figure, solid lines represent the clean (i.e., undegraded) compressor map while the dotted lines represent the degraded compressor map. Three degradation indices (degradation scaling factors), i.e., flow capacity index $SF_{c,FC}$, pressure ratio index $SF_{c,PR}$, and isentropic efficiency index $SF_{c,\text{eff}}$, defined by Eqs. (9)–(11) may be used to describe the degradation of a compressor, i.e., the shift of the characteristic speed lines.

$$SF_{c,FC} = FC_{c,\text{deg}}/FC_c \tag{9}$$

$$SF_{c,PR} = PR_{c,\text{deg}}/PR_c \tag{10}$$

$$SF_{c,\text{eff}} = \eta_{c,\text{deg}}/\eta_c \tag{11}$$

where the degradation indices are defined as the ratios between the values of degraded curves (dotted lines) and original ones (solid lines) at corresponding points. These three degradation indices are independent of each other.

At a degraded operating condition of an engine during its operation, the compressor rotational speed can be measured while the pressure ratio, mass flow rate, and isentropic efficiency can be estimated by using the performance adaptation method described in Sec. 2.1, and therefore the operating point of the compressor can be located on the compressor map as B and B' that corresponds to an operating point A and A' at the same rotational speed when the engine is clean. It can be seen in Fig. 2 that points B and B' may be at different locations on the same speed line if pressure ratio and flow capacity degrade differently. In addition, multiple solutions may be obtained if the determination of $SF_{c,PR}$ and $SF_{c,FC}$ is made only based on the location of A, A', B, and B'. To avoid multiple solutions of the degradation analysis, it is assumed that the flow capacity index is always the same as the pressure ratio index, Eq. (12), based on the fact that the degradation of pressure ratio on engine performance has similar effect to that of flow capacity degradation.

$$SF_{c,FC} = SF_{c,PR} \tag{12}$$

Based on such assumption, only two degradation indices are used to describe compressor degradation (while the pressure ratio index becomes implicit), and they are the flow capacity index $SF_{c,FC}$ and the isentropic efficiency index $SF_{c,\text{eff}}$. Point A can then be located by the intersection between a line passing through B as well as also satisfying Eq. (12) and the clean speed line at the same rotational speed. Once point A is located, corresponding point A' can be located easily on the $\eta_c - FC_c$ map, where point A' has the same rotational speed and the same mass flow rate as that of point A. Therefore the pressure ratio, mass flow rate, and isentropic efficiency at points A and A' can be determined. Due to that the same degradation indices are applied to the whole compressor map, any corresponding points on the map between clean and degraded conditions can be used to calculate the degradation indices. Therefore, the degradation indices representing the compressor degradation can be estimated with Eqs. (9)–(11) by using the values obtained at A, A', B, and B'.

2.2.2 Combustor Degradation Estimation. Combustor degradation can be represented with the degradation of combustor combustion efficiency. Combustor combustion efficiency varies with combustor load. A typical combustor characteristic map is shown in Fig. 3 where the solid line represents the combustion efficiency when combustor is clean (i.e., undegraded) while the dotted line represents the combustion efficiency when combustor is degraded. The combustor load is a function of the combustor inlet total pressure (P_b) and temperature rise across combustor (ΔT_b), Eq. (13),

$$\text{combustor load} = f(P_b, \Delta T_b) \tag{13}$$

A combustion efficiency index (combustion efficiency degradation scaling factor) is introduced to represent the degradation of a combustor and is shown in Eq. (14).

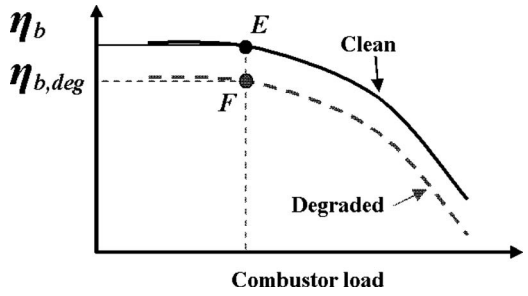

Fig. 3 Combustor characteristic map

$$SF_{b,\text{eff}} = \eta_{b,\text{deg}}/\eta_b \tag{14}$$

where $\eta_{b,\text{deg}}$ is the combustion efficiency when the combustor is degraded, and η_b is the combustion efficiency when the combustor is clean.

To obtain combustion efficiency index $SF_{b,\text{eff}}$, $\eta_{b,\text{deg}}$ is estimated with the performance adaptation method described in Sec. 2.1 when the engine is degraded. The operating point of the degraded combustor on a combustor characteristic map can be located as point F, Fig. 3, based on the value of combustor load and actual combustion efficiency $\eta_{b,\text{deg}}$. The corresponding operating point E for the same combustor load of clean combustor can be located on the combustion efficiency curve for clean combustor and therefore the combustion efficiency η_b can be obtained accordingly. Due to that the combustion efficiency index is applied to the whole combustion characteristic map, the combustion efficiency index can be estimated with the value of combustion efficiency at points F and E by using Eq. (14).

2.2.3 Turbine Degradation Estimation. Similar to the compressor degradation representation, most open literature has only mentioned turbine degradation represented by two degradation parameters relevant to turbine isentropic efficiency and flow capacity. However, the degradation of a turbine may be described more realistically by the deviation of three degradation indices relevant to its isentropic efficiency, flow capacity, and enthalpy drop. A typical turbine characteristic map is shown in Fig. 4 where the relationship among four turbine characteristic parameters, i.e., flow capacity, enthalpy drop, isentropic efficiency, and relative rotational speed, at different operating conditions is represented. In the figure, the solid lines represent the clean (undegraded) turbine characteristics while the dotted lines represent degraded characteristics. Three degradation indices may be used to describe the shift of the characteristic map due to turbine degradation, and they

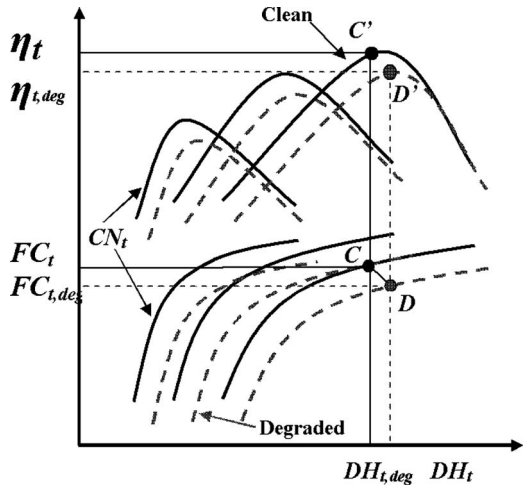

Fig. 4 Turbine characteristic map

are flow capacity index $SF_{t,FC}$, enthalpy drop index $SF_{t,DH}$, and isentropic efficiency index $SF_{t,\text{eff}}$, Eqs. (15)–(17).

$$SF_{t,FC} = FC_{t,\text{deg}}/FC_t \tag{15}$$

$$SF_{t,DH} = DH_{t,\text{deg}}/DH_t \tag{16}$$

$$SF_{t,\text{eff}} = \eta_{t,\text{deg}}/\eta_t \tag{17}$$

These three degradation indices are independent of each other.

At a degraded turbine operating condition, the turbine rotational speed can be measured while the nondimensional gas flow rate ($FC_{t,\text{deg}}$), enthalpy drop ($DH_{t,\text{deg}}$), and isentropic efficiency ($\eta_{t,\text{deg}}$) can be estimated with the performance adaptation method described in Sec. 2.1 and therefore the operating point of a turbine on the turbine characteristic map can be located as D and D' that corresponds to operating points C and C' for the clean turbine with the same rotational speed. It can be seen in Fig. 4 that points D and D' may be at different locations on the same speed line if enthalpy drop and flow capacity degrade differently. In addition, multiple solutions may be obtained if the determination of $SF_{t,DH}$ and $SF_{t,FC}$ is made only based on the location of C, C', D, and D'. To avoid multiple solutions in degradation analysis, it is assumed that the flow capacity index is inversely proportional to the enthalpy drop index, Eq. (18), based on the fact that the deviation of flow capacity and enthalpy drop has opposite effect on engine performance.

$$SF_{t,FC} = \frac{1}{SF_{t,DH}} \tag{18}$$

Based on such assumption, only two degradation indices are used to describe turbine degradation (while the enthalpy drop index becomes implicit), and they are flow capacity index $SF_{t,FC}$ and isentropic efficiency index $SF_{t,\text{eff}}$. Point C can then be located by the intersection between a line passing through D as well as satisfying Eq. (18) and the clean speed line with the same rotational speed. Once point C is located, corresponding C' can be located easily on the $\eta_t - DH_t$ map where point C' has the same rotational speed and the same enthalpy drop as that of point C. Therefore the nondimensional gas flow rate (FC_t), enthalpy drop (DH_t), and isentropic efficiency (η_t) for clean turbine at point C and C' can be determined. Due to that the same degradation indices are applied to the whole turbine characteristic map, the value of gas flow rate, enthalpy drop, and isentropic efficiency at points C, C', D, and D' can be used to calculate the degradation indices by using Eqs. (15)–(17).

2.3 Linear and Nonlinear Adaptive GPA Procedures. A typical procedure of the Adaptive GPA for the estimation of gas turbine performance and health status is shown in Fig. 5. Due to that either the linear or nonlinear performance adaptation method may be used, the approach is called linear Adaptive GPA if the linear performance adaptation is used and nonlinear Adaptive GPA if the nonlinear performance adaptation is used.

In the Adaptive GPA procedure, an accurate performance model should be created for the engine in concern at the beginning of engine operation by using advanced thermodynamic performance simulation software based on engine gas path measurements. The performance of the engine at such condition is regarded as clean engine performance, and the characteristic maps for compressors, combustors, and turbines should be an accurate description of their performance behaviors. During gas turbine engine operation, engine gas path measurements are obtained continuously and used to estimate engine performance deviation due to engine degradation by using performance adaptation techniques. In order that the gas path measurements between clean and degraded conditions are comparable, the measurements should be obtained at or corrected to the same ambient and operating condition. Once the actual engine performance status is determined, they are compared with initial clean engine performance to estimate the degra-

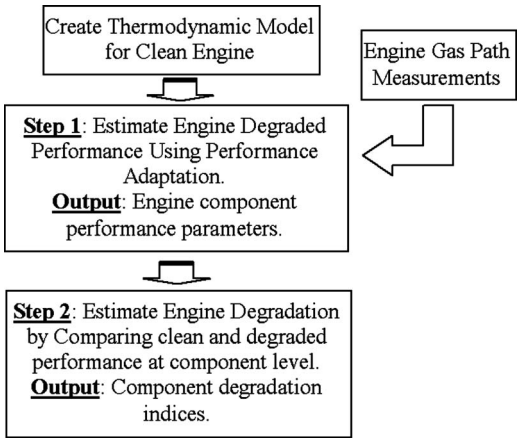

Fig. 5 Procedure of performance and health status estimation using Adaptive GPA

dation of compressors, combustors, and turbines by estimating the degradation indices of these components with Eqs. (9)–(11) and (14)–(17).

2.4 Implementation of Adaptive GPA Into PYTHIA. The developed Adaptive GPA approach has been implemented into PYTHIA [12], a software developed in the School of Engineering at Cranfield University. PYTHIA is gas turbine performance simulation and diagnostics software with a user friendly interface developed from TURBOMATCH [28]. PYTHIA provides a platform to build performance models for different gas turbine engines, to simulate gas path measurements when model engines operate at different ambient and operating conditions and at different degradation conditions, and to carry out different gas path diagnostic analyses.

3 Application and Analysis

To test the effectiveness of the developed Adaptive GPA approach, a representative model gas turbine engine similar to the Rolls-Royce aero engine Avon-300 is chosen for the demonstration of the new approach. It is a single-shaft aero turbojet engine with one compressor, one combustor, and one compressor turbine. When the engine works at certain operating conditions, the turbine entry temperature is used as a control parameter and kept constant as environmental condition changes and degradation happens. The configuration of the model engine is illustrated in Fig. 6, and the basic performance specifications of the engine are as follows [29]:

Total air flow rate	77.1 kg/s
Total pressure ratio	8.43
Turbine entry temperature	1133 K
Thrust	56.43 kN
SFC	22.94 mg/N s

The performance model for the model engine is generated using the software PYTHIA. The outputs of performance calculations are engine thrust, SFC, etc., together with the details of individual component performance and of the thermodynamic parameters at various gas path stations within the engine.

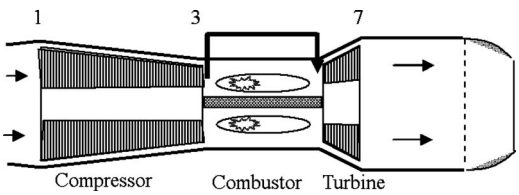

Fig. 6 Model gas turbine configuration

Table 1 Implanted degradation in three test cases

Component and health parameter		Implanted degradation (%) Test case 1	Test case 2	Test case 3
Compressor	$\Delta SF_{c,\text{eff}}$	−1.0	0	−1.0
	$\Delta SF_{c,FC}$	−3.0	0	−3.0
Combustor	$\Delta SF_{b,\text{eff}}$	0	0	−2.0
Turbine	$\Delta SF_{t,\text{eff}}$	0	−1.0	−1.0
	$\Delta SF_{t,FC}$	0	−3.0	−3.0

To test the Adaptive GPA approach for performance and health status estimation, it is assumed that the compressor, combustor, and turbine of the model engine may be degraded. The degradation of the engine is simulated by changing the degradation indices of the components defined by Eqs. (9)–(11) and (14)–(17). Three engine degradation cases shown in Table 1 are used to test the Adaptive GPA approach; the first two cases have single component degradation only, and the third case has all three major components (compressor, combustor, and turbine) degraded simultaneously. The first two cases intent to test the capability of the Adaptive GPA in isolating a degraded component and quantifying the degradation if only one component is degraded, while the third case tries to test if the approach is able to accurately predict the engine degradation if all of the major components are degraded at the same time. Once the simulated gas path measurements are collected, it is assumed that the implanted engine degradation is unknown, and the simulated measurements are used as the input to the Adaptive GPA system to test the system's capability in assessing the changing performance and health status of the engine.

The selected instrumentation set for the analysis of the model engine is described in Table 2. It is assumed that all gas path sensors are in good health (no measurement bias). It is also assumed that both clean and degraded engine performances are measured at standard ISA (International Standard Atmosphere) condition at sea level (T_{amb}=288.15 K and P_{amb}=1.0 atm). If the measurements are obtained at slightly different conditions, they should be corrected to the standard ISO condition at sea level in order that the data are comparable and can be used in the analysis. In addition, it is assumed that the nozzle area is unchanged, and the engine turbine entry temperature (TET) is kept constant at 1133 K by an engine control system when degradation happens.

The deviation of the engine gas path parameters indicates degraded engine performance. The simulated samples of those parameters are collected and regarded as simulated gas path measurements. Due to that measurement noise is inevitable in gas turbine measurements and has a negative impact on diagnostic results, they are introduced in the simulated gas path measurements to make the analysis more realistic. The simulated measure-

Table 2 Engine gas path instrumentation set

No.	Symbols	Parameters
1	T_{amb} (K)	Ambient temperature
2	P_{amb} (atm)	Ambient pressure
3	A (m^2)	Nozzle area
4	$T3$ (K)	Compressor discharge total temperature
5	$P3$ (atm)	Compressor discharge total pressure
6	$T7$ (K)	Compressor turbine exit total temperature
7	$P7$ (atm)	Compressor turbine exit total pressure
8	m_f (kg/s)	Fuel flow rate
9	CN	Shaft rotational speed relative to its design value

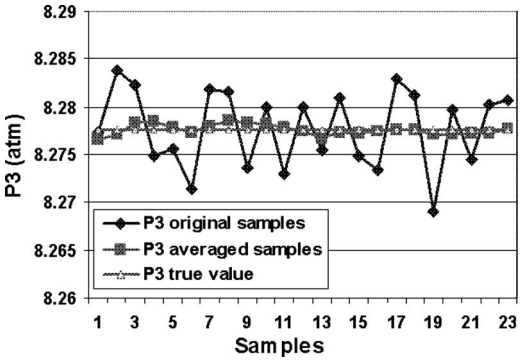

Fig. 7 Comparisons between simulated measurement samples and true values

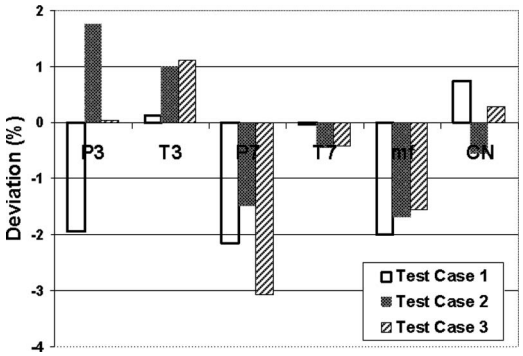

Fig. 8 Measurement deviations (i.e., fault signatures) in three test cases (T_{amb}=288.15 K, P_{amb}=1 atm, and TET is constant)

ment noise is random in quantity and follows the Gaussian distribution. The maximum measurement noise for different gas path measurable parameters is based on the information provided by Dyson and Doel [30].

To reduce the negative impact of measurement noise on performance and diagnostic analyses, multiple gas path measurement samples are obtained in the simulation, and a ten-point rolling averaging is applied to get an averaged measurement sample before the measurements are fed into the Adaptive GPA. The mathematical expression for the rolling averaging is shown in Eq. (19).

$$\bar{z}_i = \frac{1}{P}\sum_{i=1}^{P} z_i \tag{19}$$

where z_i is the gas path measurement samples, and P is the number of samples (P=10 for ten-point rolling average).

Measurement samples may be continuously obtained. The averaged sample using ten-point rolling average at a particular time is the average of the last ten samples up to that moment. An example of simulated measurement samples after data averaging and their comparisons with the true values is shown in Fig. 7.

By implanting the different degradations shown in Table 1 into the PYTHIA engine performance model, the gas path measurement deviations (fault signatures) in the three test cases are shown in Fig. 8. It shows that these engine degradations result in different engine performance deviations indicated by different gas path measurement deviations. To test the Adaptive GPA system, the gas path measurement deviations are input to the system, assuming that the degradation of the compressor, combustor, and turbine is unknown to the system.

3.1 Test Cases 1 and 2. In this study, the simulated engine performance with implanted engine degradation is called "actual performance" while the predicted engine performance by using the Adaptive GPA based on gas path measurements is called "predicted performance."

In these test cases, the two sets of measurement deviations of test cases 1 and 2 shown in Fig. 8 are input to the Adaptive GPA separately, and both the linear and nonlinear Adaptive GPAs are used to estimate the deviated engine performance and predict the corresponding engine degradation. The estimated deviated engine performance represented by the deviated value of component performance parameters and its comparison with the actual degraded performance for the two test cases are shown in Tables 3 and 4. Compared with the clean engine performance, TET is unchanged due to that it is the engine handle and kept constant by engine control system. In test case 1, engine airflow rate (ma), compressor pressure ratio (PRc), and compressor turbine isentropic efficiency (ηc) are deviated from their clean value in the quantity between -1.5% and -1.95% while the combustor combustion efficiency (ηb) and power turbine isentropic efficiency (ηt) show very little change. In test case 2, changes of -1.1%, 1.9%, -1.1%, and -0.8% happen to engine air mass flow rate (ma), compressor pressure ratio (PRc), compressor isentropic efficiency (ηc), and turbine isentropic efficiency (ηt), respectively, and almost no change to combustor combustion efficiency (ηb).

The comparison of prediction errors relative to the actual degraded performance in percentage is shown in Figs. 9 and 10 where the maximum error for the linear and nonlinear Adaptive GPAs is about 0.2% in test case 1 and about 0.3% in test case 2. It is also interesting to see that the estimated engine performance status provided by both the linear and nonlinear Adaptive GPAs is very close to each other, indicating that the linear approach is able to provide almost the same results as its nonlinear partner although it is normally believed that the nonlinear approach provides better results than its linear partner. This may be due to that this model engine performance deviates almost linearly when deg-

Table 3 Prediction of actual engine performance using linear and nonlinear Adaptive GPAs in test case 1

	Actual performance		Predicted degraded performance and its deviation from clean performance			
			From linear Adaptive GPA		From nonlinear Adaptive GPA	
	Clean	Degrade	Value	Deviation (%)	Value	Deviation (%)
ma	77.1	75.6	75.74	−1.768	75.72	−1.790
PRc	8.43	8.28	8.266	−1.945	8.266	−1.949
ηc	0.898	0.886	0.885	−1.492	0.885	−1.492
ηb	0.99	0.99	0.992	0.152	0.991	0.133
TET	1233	1233	1233.1	0.008	1233.1	0.008
ηt	0.914	0.914	0.9148	0.0875	0.9145	0.0525

Table 4 Prediction of actual engine performance using linear and nonlinear Adaptive GPAs in test case 2

	Actual performance		Predicted degraded performance and its deviation from clean performance			
			From linear Adaptive GPA		From nonlinear Adaptive GPA	
	Clean	Degrade	Value	Deviation (%)	Value	Deviation (%)
ma	77.1	76.376	76.255	−1.096	76.237	−1.119
PRc	8.43	8.591	8.586	1.854	8.586	1.854
ηc	0.898	0.890	0.888	−1.147	0.888	−1.118
ηb	0.99	0.99	0.989	−0.102	0.989	−0.118
TET	1233	1233	1234.5	0.041	1234.5	0.041
ηt	0.914	0.905	0.907	−0.781	0.907	−0.751

radation happens and also due to that the measurement noise makes the difference between the linear and nonlinear approaches invisible.

The engine component degradations in the two test cases predicted by the linear and nonlinear Adaptive GPAs are shown in Figs. 11 and 12 where the predicted deviations of all health parameters (i.e., the degradation indices) are compared with the implanted degradations. It can be seen that the predictions of the degradations from both the linear and nonlinear approaches are satisfactory, indicating that both the linear and nonlinear Adaptive GPAs are able to isolate and quantify engine component degradations satisfactorily. The maximum prediction error of degradation is around 0.24%. It also shows that the smearing effect (predicted degradation is distributed among all health parameters, although some of them are not really degraded), normally seen in some diagnostic approaches, is comparable to the level of measurement noise ($<0.4\%$) and is satisfactory even with the existence of measurement noise.

3.2 Test Case 3. In test case 3, all major engine components (compressor, combustor, and turbine) are degraded simultaneously, and the implanted degradation is shown in Table 1. The deviation of engine performance and the corresponding measurement deviation due to such degradation are shown in Fig. 8. Both the linear and nonlinear Adaptive GPAs are applied to the test case to predict both the deviated engine performance and engine degradation.

Resulted from the first step of the Adaptive GPA, a comparison among the actual clean and degraded engine performance, the predicted degraded engine performance, and its deviations from the clean performance is shown in Table 5. It can be seen that deviation of around −2.7% in engine airflow rate (*ma*), 0.2% in compressor pressure ratio (*PRc*), −2% in compressor isentropic efficiency (ηc), −1.9% in combustor combustion efficiency (ηb), and −0.7% in turbine isentropic efficiency (ηt) are predicted when TET is kept unchanged. Figure 13 shows that the maximum prediction error for performance estimation from the linear approach is about 0.23% while the maximum error for the nonlinear approach is about 0.2%. By looking at the prediction errors for all the performance parameters, it can be seen that the prediction

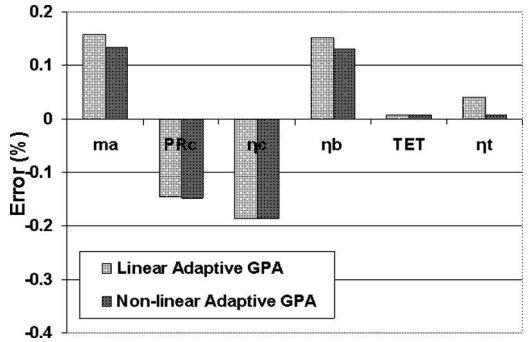

Fig. 9 Comparison of linear and nonlinear Adaptive GPA errors in test case 1

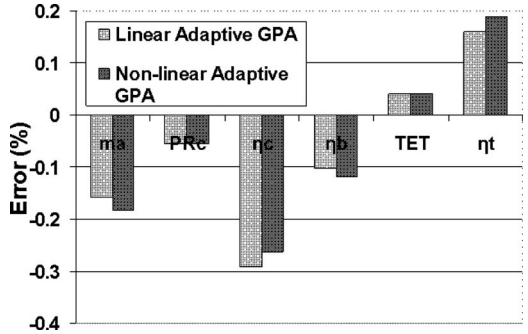

Fig. 10 Comparison of linear and nonlinear Adaptive GPA errors in test case 2

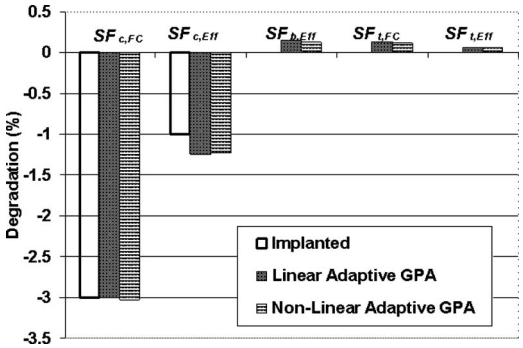

Fig. 11 Predicted degradation with linear and nonlinear Adaptive GPAs in test case 1

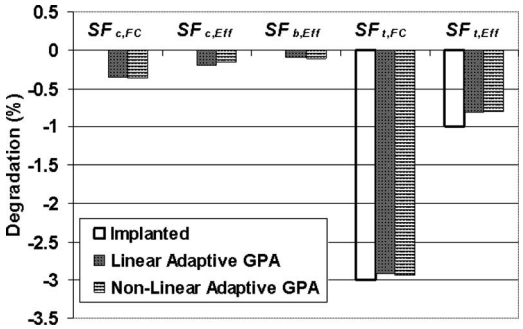

Fig. 12 Predicted degradation with linear and nonlinear Adaptive GPAs in test case 2

Table 5 Prediction of engine performance status using linear and nonlinear Adaptive GPAs in test case 3

	Actual performance		Predicted degraded performance and its deviation from clean performance			
			From linear Adaptive GPA		From nonlinear Adaptive GPA	
	Clean	Degrade	Value	Deviation (%)	Value	Deviation (%)
ma	77.1	74.97	75.03	−2.689	75.00	−2.719
PRc	8.43	8.447	8.449	0.223	8.449	0.223
ηc	0.898	0.879	0.880	−1.971	0.881	−1.915
ηb	0.99	0.97	0.972	−1.838	0.972	−1.869
TET	1233	1233	1232.6	0.049	1232.5	0.041
ηt	0.914	0.906	0.908	−0.700	0.908	−0.711

errors from the nonlinear Adaptive GPA are generally similar to that from the linear one, Fig. 13, with the existence of measurement noise.

In the second step of the Adaptive GPA, the engine component degradation predicted by the linear and the nonlinear Adaptive GPA is shown in Fig. 14 where the predicted deviations of all health parameters are compared with the implanted one. It can be seen that the predictions of the degradation from both the linear and nonlinear approaches are very satisfactory even when all three major components are degraded simultaneously. The maximum prediction error is below 0.3% for both the linear and nonlinear approaches.

3.3 Further Discussions. It can be seen in all the three test cases that the maximum prediction errors for both the performance status estimations (Figs. 9, 10, and 13) and degradation predictions (Figs. 11, 12, and 14) are comparable. Theoretically, the nonlinear approach has the potential to provide better results than its linear partner. However, with the impact of measurement noise, the slight difference in prediction accuracies is undermined.

Small smearing effect in the diagnostic results can be seen in test cases 1 and 2 (Figs. 11 and 12) where the maximum smearing effect is around −0.37%. This is also due to the negative impact of measurement noise and numerical errors of the Adaptive GPA.

With the assumptions in diagnostic analysis that the flow capacity index equals the pressure ratio index for a compressor and the flow capacity index inversely equals the enthalpy drop index for a turbine, reasonable unique solutions can be obtained from the Adaptive GPA. Although such assumptions are not ideal solutions in diagnostic analysis, it is better than not considering the pressure ratio index for compressors and the enthalpy drop index for turbines. However, such assumptions may be lifted with further investigation in this area in the future.

The computational speed of the Adaptive GPA is very fast. For example, the computational time is only a fraction of a second to get a solution with the linear Adaptive GPA and about 3 s to get a solution with the nonlinear Adaptive GPA involving 14 iterations by using a laptop computer with a 2.4 GHz dual processor. Such a calculation speed provides the possibility that the Adaptive GPA may be used in online applications. A convergence process for test case 3 is shown in Fig. 15 where the rms defined in Eq. (8) varies against the number of iterations.

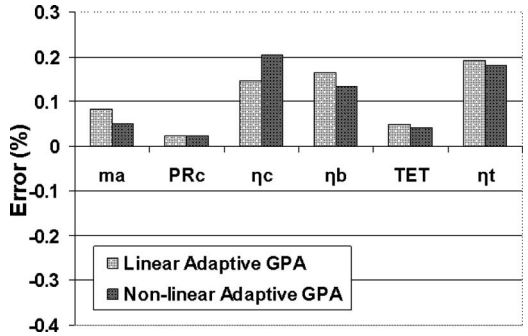

Fig. 13 Comparison of Adaptive GPA errors in test case 3

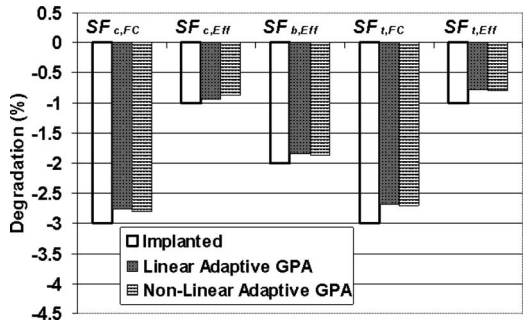

Fig. 14 Predicted degradation with Adaptive GPA in test case 3

4 Conclusions

In this study, a novel Adaptive GPA approach has been developed and presented. Such Adaptive GPA is a two step approach. The first step is the novel application of a design point performance adaptation to estimate actual performance status of a degraded engine and locate the operating point of each engine component on its component characteristic map. The second step is a novel approach introduced in this paper for gas turbine degradation analysis where the degradation analysis is done at a component level by comparing the operating point of each component when it is degraded with the operating point when it is not degraded on its characteristic map. Three degradation indices for a compressor, one for a combustor, and three for a turbine are used

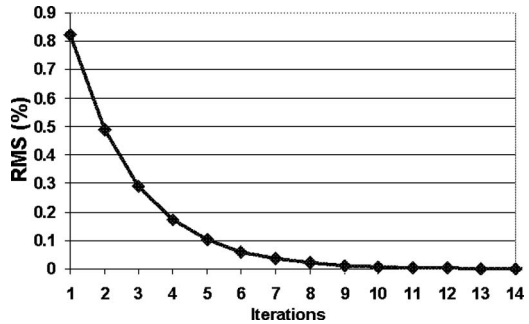

Fig. 15 Convergence process of nonlinear Adaptive GPA in test case 3

to represent different component degradations mathematically. Two assumptions, one for compressors assuming the flow capacity index being inversely equal to the pressure ratio index and the other for turbines assuming the flow capacity index being equal to the enthalpy drop index, are introduced to get reasonable unique solutions in the degradation analysis. Although such assumptions are not an ideal solution in diagnostic analysis, it is better than not considering the pressure ratio index and the enthalpy drop index. The developed Adaptive GPA approach has been applied to a model aero gas turbine engine similar to the Rolls-Royce Avon-300 implemented with degradations in three test cases—test cases 1 and 2 with single component degradations and test case 3 with all three major components (compressor, combustor, and turbine) degraded simultaneously with the existence of measurement noise to test the effectiveness of the approach. The results show that both the linear and nonlinear Adaptive GPAs have the capability to accurately predict engine performance status and engine degradation, and both approaches provide results with comparable accuracy with the existence of measurement noise. The application of the Adaptive GPA shows that the new approach has a great potential to be used in gas turbine operations to provide engine operators with the information of changing engine performance and health status based on gas path measurements. The computational speed of the approach is very fast, a fraction of second for the linear approach and few seconds for the nonlinear approach using a typical modern laptop computer, so it provides the possibility of its online applications.

Nomenclature

- A = nozzle cross area (m^2)
- CN = shaft rotational speed relative to its design value (%)
- DH = enthalpy drop
- FC = flow capacity
- H = Influence Coefficient Matrix (ICM)
- M = number of measurement parameters
- m_a = engine air flow rate (kg/s)
- m_f = fuel flow rate (kg/s)
- N = number of engine component parameters
- P = total pressure (atm)
- PR = pressure ratio
- SF = degradation index or degradation scaling factor
- SFC = specific fuel consumption (mg/N s)
- T = total temperature (K)
- TET = turbine entry temperature (K)
- $\vec{x}$ = engine component performance parameter vector
- $\vec{z}$ = engine gas path measurement parameter vector
- Δ = deviation
- σ = convergence threshold
- η = efficiency

Subscripts

- amb = ambient
- b = combustor
- c = compressor
- DH = enthalpy drop
- deg = degraded condition
- eff = isentropic efficiency
- FC = flow capacity
- PR = pressure ratio
- t = turbine
- 0 = clean (or undegraded) condition
- 1 = engine inlet
- 3 = compressor exit
- 7 = compressor turbine exit
- # = pseudo-inverse

References

[1] Roth, B. A., Mavris, D. N., and Doel, D. L., 2003, "Estimation of Turbofan Engine Performance Model Accuracy and Confidence Bounds," 16th International Symposium on Air Breathing Engines, ISABE Paper No. 2003-1208.

[2] Roth, B. R., Mavris, D., Doel, D. L. and Beeson, D., 2003, "High-Accuracy Matching of Engine Performance Models to Test Data," ASME Paper No. GT2003-38784.

[3] Li, Y. G., Pilidis, P., and Newby, M. A., 2006, "An Adaptation Approach for Gas Turbine Design-Point Performance Simulation," ASME J. Eng. Gas Turbines Power, **128**, pp. 789–795.

[4] Li, Y. G., 2008, "A Genetic Algorithm Approach to Estimate Performance Status of Gas Turbines," ASME Paper No. GT2008-50175.

[5] Urban, L. A., 1972, "Gas Path Analysis Applied to Turbine Engine Condition Monitoring," Paper No. AIAA-72-1082.

[6] Doel, D. L., 1994, "An Assessment of Weighted-Least-Squares-Based Gas Path Analysis," ASME J. Eng. Gas Turbines Power, **116**, pp. 366–373.

[7] Borguet, S., and Leonard, O., 2009, "A Generalized Likehood Ratio Test for Adaptive Gas Turbine Performance Monitoring," ASME J. Eng. Gas Turbines Power, **131**, p. 011601.

[8] Romessis, C., and Kamboukos, Ph., and Mathioudakis, K., 2007, "The Use of Probabilistic Reasoning to Improve Least Squares Based Gas Path Diagnostics," ASME J. Eng. Gas Turbines Power, **129**, pp. 970–976.

[9] Volponi, A. J., 1982, "Gas Path Analysis: An Approach to Engine Diagnostics," 35th Symposium Mechanical Failures Prevention Group, Gaithersburg, MD, Apr.

[10] Provost, M. J., 1988, "COMPASS: A Generalized Ground-Based Monitoring System," Engine Condition Monitoring—Technology and Experience, Oct., Paper No. AGARD-CP-449.

[11] Escher, P. C., and Singh, R., 1995, "An Object-Oriented Diagnostics Computer Program Suitable for Industrial Gas Turbines," 21st (CIMAC) International Congress of Combustion Engines, Switzerland, May 15–18.

[12] Li, Y. G., and Singh, R., 2005, "An Advanced Gas Turbine Gas Path Diagnostic System—PYTHIA," ISABE, Munich, Germany, Sept., Paper No. ISABE-2005-1284.

[13] Denney, G., 1993, "F16 Jet Engine Trending and Diagnostics With Neural Networks," Proc. SPIE, **1965**, pp. 419–422.

[14] Ogaji, S. O. T., and Singh, R., 2003, "Gas Path Fault Diagnosis Framework for a Three-Shaft Gas Turbine," Proc. Inst. Mech. Eng., Part A, **217**, pp. 149–157.

[15] Tan, H. S., 2006, "Fourier Neural Networks and Generalized Single Hidden Layer Networks in Aircraft Engine Fault Diagnostics," ASME J. Eng. Gas Turbines Power, **128**, pp. 773–782.

[16] Romessis, C., and Mathioudakis, K., 2006, "Bayesian Network Approach for Gas Path Fault Diagnosis," ASME J. Eng. Gas Turbines Power, **128**, pp. 64–72.

[17] Zedda, M., and Singh, R., 2002, "Gas Turbine Engine and Sensor Fault Diagnosis Using Optimization Techniques," J. Propul. Power, **18**(5), pp. 1019–1026.

[18] Gulati, A., Zedda, M., and Singh, R., 2000, "Gas Turbine Engine and Sensor Multiple Operating Point Analysis Using Optimization Techniques," Paper No. AIAA-2000-3716.

[19] Wallin, M., and Grönstedt, T., 2004, "A Comparative Study of Genetic Algorithms and Gradient Methods for RM12 Turbofan Engine Diagnostics and Performance Estimation," ASME Paper No. GT2004-53591.

[20] Ganguli, R., 2001, "Application of Fuzzy Logic for Fault Isolation of Jet Engines," ASME Paper No. 2001-GT-0013.

[21] Martis, D., 2007, "Fuzzy Logic Estimation Applied to Newton Methods for Gas Turbines," ASME J. Eng. Gas Turbines Power, **129**, pp. 88–96.

[22] Eustace, R., 2008, "A Real-World Application of Fuzzy Logic and Influence Coefficients for Gas Turbine Performance Diagnostics," ASME J. Eng. Gas Turbines Power, **130**, pp. 061601.

[23] Li, Y. G., 2003, "A Gas Turbine Diagnostic Approach With Transient Measurement," Proc. Inst. Mech. Eng., Part A, **217**, pp. 169–172.

[24] Surender, V. P., and Ganguli, R., 2005, "Adaptive Myriad Filter for Improved Gas Turbine Condition Monitoring Using Transient Data," ASME J. Eng. Gas Turbines Power, **127**, pp. 329–339.

[25] Li, Y. G., 2002, "Performance-Analysis-Based Gas Turbine Diagnostics: A Review,"Proc. Inst. Mech. Eng., Part A, **216**(A5), pp. 363–377.

[26] Singh, R., 2003, "Advances and Opportunities in Gas Path Diagnostics," 15th ISABE, Paper No. ISABE-2003-1008.

[27] Jaw, L. C., 2005, "Recent Advances in Aircraft Engine Health Management (EHM) Technologies and Recommendations for the Next Step," ASME Paper No. GT2005-68625.

[28] Macmillan, W. L., 1974, "Development of a Modular Type Computer Program for the Calculation of Gas Turbine Off Design Performance," Ph.D. thesis, Cranfield University, Bedford, UK.

[29] Gunston, B., 2006, *Jane's Aero-Engines*, Issue 20, pp. 496, printed by Hobbs the Printer.

[30] Dyson, R. J. E., and Doel, D. L., 1987, "CF-80 Condition Monitoring—The Engine Manufacturing's Involvement in Data Acquisition and Analysis," Paper No. AIAA-84-1412.